International Journal of Environmental Sciences
ISSN: 2229-7359
Vol. 11 No. 17s,2025
https://theaspd.com/index.php

Green Synthesis and Characterization of Silver Nano Particles from *Cleome felina* and Its Anti Microbial Properties

K. Vijay Kumar*[1] and S. Kavitha[2]

[1]Research scholar, Dept. of Chemistry, Chaitanya (Deemed to be University), Near Chilukuri Balaji Temple, Himayatnagar, Hyderabad, Telangana, India, vijaychemstar@gmail.com

[2]Professor, Dept. of Chemistry, Chaitanya (Deemed to be University), Near Chilukuri Balaji Temple, Himayatnagar, Hyderabad, Telangana, India.

Abstract

Silver nanoparticles (AgNPs) have garnered considerable interest due to their antibacterial capabilities. This research examines the eco-friendly synthesis of silver nanoparticles (AgNPs) utilizing Cleome felina (Cleomaceae) leaf extract, which serves as both a reducing and stabilizing agent. The synthesis of AgNPs was validated by a colour shift and characterized using UV-Vis spectroscopy, FTIR, SEM, TEM, XRD, and zeta potential analysis. UV-Vis spectroscopy revealed a peak at 302 nm, indicating nanoparticle production, whereas FTIR detected functional groups important for stabilization. SEM and TEM investigations demonstrated primarily spherical nanoparticles with an average diameter of 15 nm, while XRD validated their crystalline structure.

The antibacterial efficacy of AgNPs produced from C. felina was assessed against the bacterial strains Staphylococcus aureus, Streptococcus pneumoniae, Escherichia coli, and Pseudomonas aeruginosa. The nanoparticles demonstrated dose-dependent antibacterial activity, with the highest inhibition recorded against E. coli (14 mm) and P. aeruginosa (14 mm). Minimum Inhibitory Concentration (MIC) analyses validated their bacteriostatic efficacy. Furthermore, antifungal efficacy was evaluated against Candida albicans and Aspergillus niger, demonstrating modest inhibition relative to fluconazole, with maximum inhibition zones of 13 mm and 8 mm, respectively. These findings underscore the promise of Cleome felina-derived AgNPs as an environmentally sustainable antibacterial agent, especially against Gram-negative bacteria. Additional research is required to investigate their clinical applications and improve stability.

Keywords: *Silver nanoparticles, Synthesis, Cleome felina, Cleomaceae, Antimicrobial*

INTRODUCTION

The revolution in nanotechnology has marked a significant turning point in history. Nanotechnology involves the manufacturing, manipulation, and imaging of nanostructures with sizes ranging from 1 to 100 nm (Kumar et al., 2017). The idea of nanotechnology was first proposed by Feynman in 1959. Nanotechnology has created new opportunities in several industries, such as food packaging, animal husbandry, electronics, agriculture, medicine, and health care. It is also one of the most recent industrial developments (Balachandar et al., 2019).

The quest for novel nanomaterials and production techniques is becoming more and more frenzied as nanotechnology, which is the fastest-growing sector in this world today (Quazi et al., 2023, Singh et al., 2019, Yaqoob et al., 2020). When compared with its larger counterpart (Bulk), nanoparticles have distinctive physical, chemical and biological characteristics due to their small size and large surface area, which led to improved interaction or stability during the physical and chemical process, increased mechanical strength and other factors (Khan, et al., 2019; Baig et al., 2021; Sabouri et al., 2020). Nanotechnology is rapidly developing, and many intensive studies have been conducted to synthesize nanoparticles with distinctive characteristics in terms of cost, speed of completion and the distinctive characteristics of the resulting nanoparticles8. NPs have been used in a variety of applications including cooking utensils, renewable energies, agricultural pest control and have been used extensively in the medical field, treating a wide range of diseases, as well as transporting medicines and improving the quality of materials (Tulli, et al., 2022). Nanoparticles have significant applications in different sectors such as the environment, agriculture, food, biotechnology, biomedical, medicines, etc. like; for treatment of waste water (Zahra et al., 2020), environment

monitoring (Rassaei et al., 2011), as a functional food additive (Chen et al., 2023), and as a antimicrobial agents (Islam et al., 2022). Cutting-edge properties of NPs such as; nature, biocompatibility, anti-inflammatory and antibacterial activity, effective drug delivery, bioactivity, bioavailability, tumor targeting, and bio-absorption have led to a growth in the biotechnological, and applied microbiological applications of NPs. Top-down and bottom-up approaches can be used for the synthesis of AgNPs. The top-down approach involves breaking down a bulk material into nano-sizes using techniques such as laser ablation and puttering. In contrast, the bottom-up approach refers to building nanoparticles using smaller entities, such as chemical and biological methods (Varadan et al., 2010). Green synthesis of nanomaterials is an excellent alternative to developing recyclable nanomaterials that are non-toxic through methods that give minimal waste byproducts. Green synthesis methods thus involve eco-friendly methods for nanomaterial synthesis. Recently, multiple biological substrates like bacterial components, fungi, and plant extracts have been employed to synthesize metal and metal oxide-based nanomaterials. However, several external parameters like the temperature, pH, pressure, and the chemicals used must be considered before switching to the 'green method' of synthesis of nanoparticles. The development of metal and metal oxide-based nanomaterials depends on phytochemicals present in the plant leaves, like carboxylic and ascorbic acids, alkaloids, ketones, flavonoids, aldehydes, tannins, amides, and phenols, among others. These chemicals have the potential to give metal nanoparticles by the reduction of metal salts (Singh et al., 2018). Furthermore, plant derived nanoparticles benefit from the bio-reducing agent from the plant sources including the capping agents like phytochemicals that enhance the overall biocompatibility of the synthesized nanoparticles (Rajan et al., 2015). Green synthesis of nanoparticles also confers additional advantages as compared to the chemical synthesis of nanoparticles including the increase in half-life of the nanomaterial, higher efficiency and therefore are lesser toxic and more biocompatible (Adeyemi et al., 2022). Therefore, nanomaterial synthesis using a plant source is advantageous because the entire synthesis process is quicker, cheaper, and involves simpler processes than other conventional methods (Bao et al., 2021).

Silver nanoparticles (AgNPs), among other nanoparticles, have received extensive attention because of their unique properties (Bindhu et al., 2015; Marimuthu et al., 2011; Sharma et al., 2009; Velusamy et al., 2015; Verma & Mehata, 2016). AgNPs are essential nanomaterials studied extensively because of their electrical, optical, and biological properties. Consequently, these nanoparticles have been used for numerous applications, including biosensing, drug delivery, nanodevice fabrication, and medicine (Jain et al., 2008). Biological processes, known as green synthesis, primarily conducted *via* medicinal plants, offer advantages over chemical and physical methods because they are cost-effective, eco-friendly, and readily available. This manuscript reviews the recent developments in green synthesis, optimization conditions, mechanisms, and characterization techniques for AgNPs, particularly using medicinal plant extracts, and discusses the effects of different parameters on green synthesis. Standard characterization techniques include ultraviolet–visible (UV–Vis) spectrophotometry, Fourier transform infrared (FTIR) spectroscopy, scanning electron microscopy (SEM), transmission electron microscopy (TEM), dynamic light scattering (DLS), X-ray diffraction (XRD), and zeta potential analysis.

The genus *Cleome* is reported to possess pharmacologically active phytocompounds, which have been isolated, as they perform a vital role in the treatment of several ailments. The various plant parts of the genus *Cleome* have revealed good nutritional and therapeutic value. The most important class of secondary phyto-compounds has been derived from the *Cleome* species, which includes terpenes, sterols, flavonoids, glucosinolates, indole alkaloids, and isothiocyanates, which are distributed in various *Cleome* species (Chand, et al., 2022; Singh et al., 2018). *Cleome felina* is one among the species of the genus *Cleome*, it is belonging to the family Cleomaceae, which is a medicinal plant and is endemic to peninsular India (Hanumantha Rao, 2016). It is annual hairy herb is 30–60 cm, with trifoliate leaves, corolla pink, and more than 50 stamens; seedpods with seeds are slightly longer than the pedicel and is widely distributed in Deccan districts of Madras Presidency. (Joseph et al., 2014).

C. felina fresh and dry portions are advised for epistaxis; they are mashed in equal amounts and administered with milk and sugar. Internal administration of the vesicant seeds as a vermifuge and the entire plant as an astringent (Manjuparkavi and Jayanthi 2019). The plant is used as an astringent (Nadkarni, 1954). The seeds are vesicant and given internally as vermifuge (Henri Baillon, 1874). According to Nicola et al., (1996) reported anti-cancer properties, preventing tumor formation through decreasing inflammation and tumor growth of *C. felina.* According *to* Joseph et al., (2014) also evaluated the antineoplastic activity of an ethanol extract of *C. felina* leaves. The anticancer effects were analyzed using the 3-(4,5-dimethylthiazol-2-yl)-2,5-diphenyltetrazolium bromide (MTT) assay against HepG2 (human hepatocellular liver carcinoma cell line) cells. Maximum inhibition of cell growth was noticed at a concentration of 200 µg/mL.

Shaikh et al., (2023) reported antimicrobial assay showed a moderate zone of inhibition against *S. aureus*, *B. cereus*, *E. coli*, *P. aeruginosa*, *C. albicans*, and *C. glabrata* at 100 µL/mL concentration.

A review of the literature indicates that, to date, no research has been conducted on the synthesis and characterization of silver nanoparticles (AgNPs) and the antimicrobial activities of *Cleome felina*. This study emphasized on the green synthesis and characterization of AgNPs utilizing *C. felina* aqueous extract as both a reducing and stabilizing agent. The synthesized AgNPs will undergo characterization through UV-Visible spectroscopy, FT-IR, SEM, ZP, and TEM techniques. Additionally, the antimicrobial properties of synthesized silver nanoparticles will be assessed against various human pathogens.

Materials and methods

Plant material

The plant leaves from *Cleome felina* L.f. (*Cleomaceae*) about 1kg, were collected from Sriramgiri (located **17.591306**°N, **79.82429**°E) Village, Nellikudur Mandal, Mahabubabad District, Telangana state, India, during August / September in the year 2023.

Authentication of Cleome *felina*

The plant was taxonomically identified and authenticated by Botanical Survey of India Deccan Regional Centre, Hyderabad, Telangana, India, (Voucher Number-. (BSI/DRC/2023-24/Identification/732), and the specimen deposited at Herbarium, Hyderabadensis, Department of Botany, O.U, Hyderabad, Telangana, India.

Drying

The collected plant materials have been washed with double-distilled water. The plant leaves were air-dried at room temperature for no more than of three weeks and subsequently pulverized into a fine powder.

Successive extraction using Soxhlet apparatus

In order to properly prepare the *C. felina* leaf extract, fresh leaves were obtained and thoroughly cleaned by cleaning them with the flow of water. This procedure was carried out to completely eradicate any particles or contaminants that might have been present. An aqueous solution has been used for the extraction of the leaves. The dried leaves performed grinding into a powder utilizing a mechanical grinder, followed by sieving to ensure the powder maintained a consistent particle size throughout. The extraction of leaf powder was conducted incrementally at a temperature of 100°C utilizing water and the Soxhlet apparatus. The extract underwent filtration using Whatman No. 1 filter paper to obtain a particle-free solution (Anandalakshmi et al., 2016).

Preparation of silver nitrate solution

0.01697 g of $AgNO_3$ was dissolved in 100 mL distilled water to produce 1 mM solution of $AgNO_3$.

Preparation of 0.1 M NaOH solution

0.4 g of NaOH was dissolved per 100 mL of distilled water to prepare 0.1 M NaOH solution and further used to adjust the pH values in different experiments.

Green synthesis of silver nanoparticles

Synthesis of silver nanoparticles using leaf extract

A solution of 90 mL of double-distilled water containing 1 mM silver nitrate was used to form the silver nanoparticles, to which 10 mL of *C. felina* leaf extract was subsequently added. The leaf extract was mixed

with silver nitrate in a ratio of 1:9. The reaction mixture was heated to 80 °C with a magnetic stirrer and stirred continuously for three hours at an acceleration of 800 rpm. The shift in colour from yellow to dark brown signified the development of AgNPs. A suspension of AgNPs-*C. felina* was prepared and subsequently centrifuged at 15,000 rpm for 45 minutes. To remove the silver ions and residual leaf extract, the pellet containing the silver nanoparticles was subjected to a comprehensive rinsing process with deionized water, repeated three to four times. The formed nanoparticles underwent freeze-drying. The lyophilized nanoparticles were subjected to further characterization after being stored in a cool, dry, and dark environment. The silver nanoparticles, synthesized using a green method and tagged, were kept at a temperature of 4 °C until further experimental analysis. (Pal et al., 2017).

Silver nanoparticles synthesis at varying PH

To enable the formation of silver nanoparticles throughout different levels of pH, that range from 3 to 11, the solutions were prepared with a constant concentration (15 mL leaf extract) at 80 °C in both acidic and basic conditions. Glacial acetic acid was added dropwise to decrease the pH, while sodium hydroxide was added dropwise to increase it.

Characterization of AgNPs - *C. felina*

The synthesized AgNPs of *C.felina* leaf extracts were characterized by UV-Vis- spectroscopy (UV-Vis), Fourier-transform infrared spectroscopy (FTIR), Scanning Electron Microscopy (SEM), X-ray powder diffraction (XRD) and Zeta Potential (ZT).

UV–visible spectroscopy

This method is mostly employed to monitor and evaluate the stability and synthesis of metallic nanoparticles for characterization purposes. The primary method utilized for nanoparticle characterization is UV–visible spectroscopy (Astry, 1998). Vanden Bout et al. (2011) showed that the principal absorbance peak in UV-vis spectra correlates with the surface plasmon resonance (SPR) of silver nanoparticles. The UV–visible spectra of stable silver nanoparticles and the aqueous extract of fresh AgNPs - *C. felina* was recorded using a UV–vis spectrometer (Shimadzu Japanese UV-2450) with a resolution of 1 nm. AgNPs - *C. felina* extracts were used as a reducing agent. The samples were analyzed at the ambient temperature within the wavelength range of 300–800 nm at a scanning rate of 475 nm per minute, using a 1 cm optical path. UV–vis absorption spectra were obtained 24 hours after incubating the $AgNO_3$ solution with *C. felina* leaf extract. One possible cause of yellowing in the backdrop is the use of distilled water (Vanden Bout et al., 2011). This is the typical range of wavelengths used to describe nanoparticle production and assess the optical properties of AgNPs. The study of the UV-vis spectra allowed for a more complete understanding of the nanoparticle synthesis process. These spectra confirmed the effective synthesis of silver nanoparticles and provided details about their size distribution and morphology.
(Straková et al., 2020).

Fourier Transforms Infrared Spectroscopy (FTIR)

The AgNPs solution was centrifuged for 30 minutes at 10,000 rpm. Three or four thorough washes of the supernatant solution were conducted in order to eliminate any unbound proteins or enzymes that are not capping the AgNPs. A vacuum drier was used to dry the pellet.

A dry leaf powder of *C. felina* leaf extract was obtained and measured at a resolution of 4 cm-1 utilizing the diffuse reflection mode of the potassium bromide (KBr) pellet technique in Fourier transform infrared (FTIR, Dept. of Analytical and Structural Chemistry, CSIR-Indian Institute of Chemical Technology (CSIR-IICT), Hyderabad, Telangana, India) spectroscopy. An infrared light with a wavelength of 500–4000 cm–1 was used to mix the powder with KBr. For the FTIR analyses of AgNPs- *C. felina* leaf extract prior to and following bio reduction, a comparable procedure was employed (Pakkirisamy et al., 2017; Eid, 2022). The force constant and reduced mass are the two factors that determine the frequency of the vibrational peak (ν), and these factors can be expressed by the following equation (Ahmed et al., 2021; Al-Otibi et al., 2021).

$$\nu = 1/2\pi c \sqrt{(k/\mu)}$$

Here ν - is the speed of light,

k- is the force constant
μ- is the reduced mass

Scanning Electron Microscope (SEM)

A scanning electron microscope that was produced in Germany and had EDS-Mapping-Line-EBSD capabilities was used to analyze the structure and size of silver nanoparticles. The material was put through centrifugation at a rotation speed of 10,000 revolutions per minute for 15 minutes in order to conduct the evaluation. After that, the sample was rinsed with distilled water and dried at a temperature of 50 degrees Celsius. The sample was placed on a platinum mesh that had been coated with palladium. The sample was then analyzed using radiation that flowed through it. The image that was produced showed a dispersion spectrum with an energy of 250 INCA. (Amargeetha and Velavan, 2018; Nasiriboroumand et al.,2018).

Transmission Electron Microscopy (TEM)

The structural and morphological characterization of silver nanoparticles (AgNPs) was carried out using Transmission Electron Microscopy (TEM) according to published techniques (Kumar et al., 2021; Zhang et al., 2020) The sample was prepared by micro pipetting a tiny volume of colloidal silver nanoparticle suspension onto a carbon-coated copper grid to ensure uniform dispersion. To prevent aggregation and improve image quality, filter paper thoroughly removed excess water. Before microscopy, the grid was air-dried at room temperature for 5–10 minutes. Our US-made FEI Tecnai G2S Twin TEM high-resolution transmission electron microscope evaluated the dehydrated samples. Imaging at various magnifications assessed nanoparticle size, shape, and lattice structure. Nanoparticle resolution and clarity increased by optimizing electron beam intensity, focus, and contrast. Lattice fringe analysis using highest-resolution transmission electron microscopy (HRTEM) revealed silver nanoparticle crystallinity, interplanar spacing, and atomic structure. Particle size distribution and possible agglomeration were analyzed to assess nanoparticle homogeneity and stability. Singh & Mehta (2019) state that nanoparticle characterization requires high-resolution transmission electron microscopy (TEM) images to assess structural characteristics. In biomedical research, antimicrobial coatings, drug delivery, and nano catalysis, silver nanoparticles' physicochemical qualities depend on structural and morphological characterization using TEM (Wang et al., 2018).

X- ray Diffraction

The crystal structure and size of the sample was studied by X-ray Diffraction. About 1 ml of colloidal AgNps was uniformly spread on glass plate and kept to dry in an oven. This process was repeated 2-3 times in order to get a thin film on plates. Before spreading nanoparticles, glass plates were properly washed with acetone and ethyl alcohol in the sonicator. XRD spectra of the resulted AgNps were measured on Rigaku-Ultima IV X-ray Diffractometer (operating at 40 kV voltage and 30 mA current with Cu k (radiations (λ1 = 1.54056; λ2 = 1.54439). For this analysis, thin film of AgNps on glass slides was placed in diffraction arm. The diffracted intensities of the sample were recorded at 2 angles ranging from 30 degrees to 80 degrees (Kamble, et al.,2022). The size of the crystalline AgNPs was calculated using Debye-Scherrer equation, i.e. =

$$D = {K\lambda}/{\beta\cos\theta}$$

Where, D = Crystalline size of nanoparticles
K = crystalline-shape factor
λ = X-ray wavelength
β = X-ray diffraction broadening, radian
θ = observed peak angle in degree

Zeta potential measurement

The surface electric charge of Ag NPs was established by detecting the particles that are most stable when there is electrostatic repulsion between them. The determination of zeta potential was carried out using the HAS 300 instrument, which is based on photon correlation spectroscopy (Kibiti and Afolayan, 2015). The

analysis duration was 60 seconds, during which the average zeta potential was measured. The dispersion was determined without any dilution.

Antibacterial activity (Bhandari et al., 2023; Meri Amerikova et al., 2019)

Bacterial Strains:

The bacterial strains Gram positive of *Staphylococcus aureus* (ATCC 25923)*, Streptococcus pneumonia* (ATCC 33400)*,* and Gram negative of Pseudomonas *aeruginosa* (ATCC 27853) *, E. coli* (ATCC 25922) used in the study were obtained from ATCC.

Media Preparation for Anti-Bacterial Activity:

A) Nutrient Agar Media

Nutrient Agar we procured from commercially and weighed 28.0 gms of powder dissolved in 1000 ml distilled water and mix thoroughly. Sterilized the dissolved nutrient agar in autoclave at 121^0 C for 15 mins and used the media for plate preparation to study the anti-bacterial activity.

B) Nutrient Broth

Nutrient Broth we procured from commercially and weighed 1.3 gms of powder dissolved in 100 ml distilled water and mix thoroughly. Sterilized the dissolved nutrient broth in autoclave at 121^0 C for 15 mins and used the broth for inoculum preparation.

C) Preparation of stock solution:

The stock culture of each organism was prepared by taking two nutrient agar slants and sub culturing each confirmed test organism aseptically. One set slant was kept as stock culture and another as working set. The cultures of bacteria in their appropriate agar slants were stored at 4°C and used as stock cultures. One counter glycerol stock was also maintained at 20° C temperature.

D) Inoculum preparation:

The selected bacterial pathogens were inoculated into nutrient broth and incubated at 37°C for 24 hours and the suspensions were checked to provide approximately 10-5 CFU/ml.

Antibacterial activity AgNPs- CFL

Anti-bacterial activity of nano particles sstudied by the Agar well-diffusion method with four concentrations (25, 50,75 and 100 µl) were tested against bacterial pathogens such as of *Staphylococcus aureus, Streptococcus pneumonia,* Pseudomonas *aeruginosa* and *E. coli*.The plates were incubated at 37°C for 18-24 hrs and end of the experiment the diameter of the inhibition zone (mm) was measured and the activity index was also calculated. The readings were taken in three different fixed directions and the average values were recorded.

Minimum Inhibitory Concentration (MIC) (Sumaiya Naeema et al., 2023)

Minimum Inhibitory Concentration (MIC), is the lowest concentration of an anti-microbial growth that will inhibit the visible growth of a microorganism after overnight incubation.

Extract Preparation:

Extracts were weighed individually 1mg and dissolved in methanol for final stock concentration as 1mg/ml. As same sample, standard ampicillin also prepared.

Culture Preparation:

Loop of culture was inoculated in 3 ml of nutrient broth and incubate 37 ^{0} c for overnight in shaking incubator.

Inoculum Preparation:

From overnight grown culture, 20 µl of culture was taken and inoculated in 1.5 ml of nutrient broth and added different concentration of compound and incubated at 37 ^{0} c for overnight in an incubator.

Anti-Fungal Activity (Nair et al., 2014)

Fungal Strains:

The fungal strains *Candida albicans* (MTCC 183) and *Aspergillus niger* (MTCC) used in the study was obtained from Microbial type culture collection (MTCC), Institute of Microbial Technology (IMTECH), Chandigarh

Sabouraud Dextrose Agar (SDA):
Sabouraud dextrose agar procured commercially and weighed 32.5 gms of powder dissolved in 500 ml distilled water and mix thoroughly. Sterilized the dissolved SDA in autoclave at 121^0 C for 15 mins and used the SDA for the plate preparation to study the anti-fungal activity.

Antifungal activity of AgNPs - CFL

Anti-fungal activity was tested by well diffusion method w. The prepared SDA culture plates were spreader with *Candida albicans* and *Aspergillus niger* fungus using spread plate method. The plates were incubated at 37+2ºC for 48 hrs for fungal activity. After 48 hrs, the plates were observed for zone formation around the well and the zone of inhibition (mm) was measured.

RESULTS

Morphological description of *C. felina*

Annual herbs, about 15-50 cm tall. Stem erect or decumbent, woody at the base simple or branched, densely strigose appressed hairs, branches slender, usually branched from the base. Leaves tri-foliate, uppermost leaves simple or uni-foliate, leaflets sessile, covered with rigid scale like hairs, oblong-obovate, middle leaflets about 15-25 x 7-15 mm across, base cuneate, margin ciliate, apex rounded, lateral leaflets 5-15 x 3-12 mm across, petiole about 1-2 cm long, near the base, becoming shorter and subsessile upwards. Inflorescence racemes, solitary, lax and elongated in fruit, axillary. Flowers bisexual, zygomorphic, pink or purple, about 5-8 mm across, pedicel filiform, slender, about 10-15 mm long, elongating up to 22 mm long in fruit, sepals 4, equal, linear lanceolate, valvate, free or slightly fused at the base, slightly connate at the base, apex subacute, scabrid, about 4-5.5 x 0.5-1 mm across, petals 4, elliptic obovate to spathulate, pubescent outside, about 8-11 x 1.5-3.5 mm across. Stamens 25-40, filament inserted on a discoid, purple or violet, about 3-4 mm long, anthers ovoid. Ovary superior, bicarpellary, sessile, about 5-6 mm long, 3-5 mm thick, ovules many on parietal 2 placentae. Fruit capsule, dehiscent, linear cylindric, about 20-30 x 2-3 mm across, beaked at apex, with persistent seed-bearing replum. Seeds many, orbicular or reniform, about 1.5-2.5 mm across, cleft fused between 2 ends, surface smooth, yellowish brown **(Fig1 A-D).**

Fig1A-D: Habitat of *C. felina*

International Journal of Environmental Sciences
ISSN: 2229-7359
Vol. 11 No. 17s,2025
https://theaspd.com/index.php

Distribution of *C. felina*

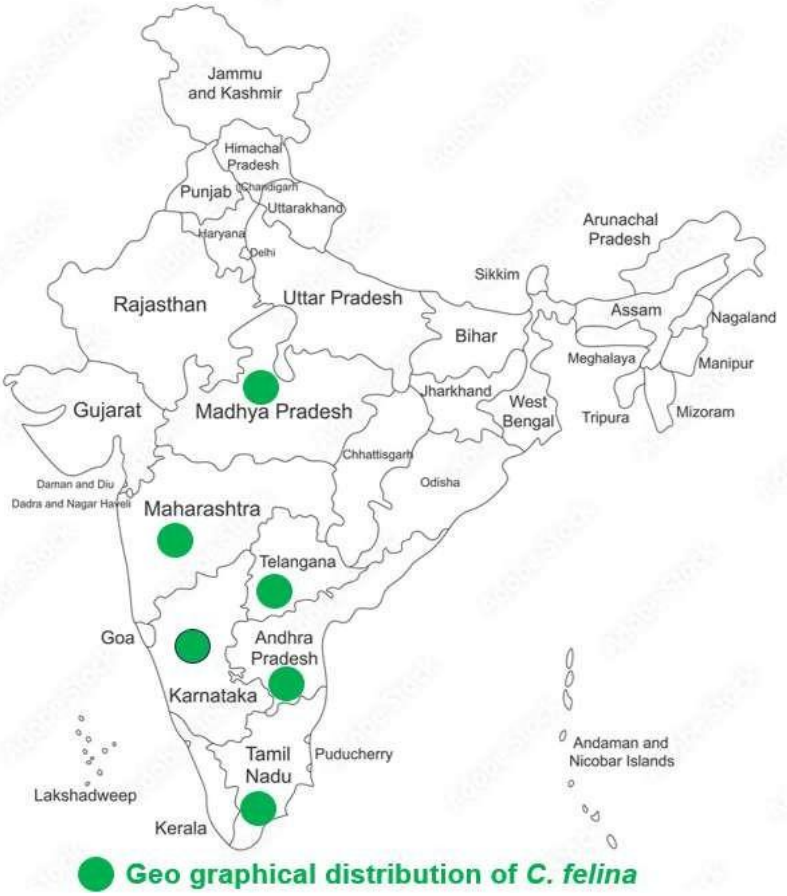

Fig.2: Distribution of *C. felina*

Synthesis of Ag-NPs of *C. felina*

Using silver ions (Ag+) and *C. felina* leaf extract, a reduction method was employed to fabricate silver nanoparticles (AgNPs). The plant extract serves an eco-friendly purpose as it functions as both a stabilizing and reducing agent, easing the transition of Ag+ ions into Ag metal. To begin the process, 10 mL of *C. felina* leaf extract was added to 90 mL of 1mM aqueous solution of AgNO3. During the reaction, a heat of 80 °C with constant stirring and 3-hour duration guaranteed a positive interaction between silver ions and biomolecules. The process is marked using color change where the conversion of Ag+ ions into Ag+ ions changes the appearance from yellow to dark brown. The resulting exhibit of exciting surface plasmons or SPR within the synthesized silver nanoparticles attributed the obtained result to electrochemistry. With regards to UV-Vis Spectroscopy, AgNPs were made using a well-defined SPR band of 445 NM. The synthesized nanoparticles were labeled and stored at 4^{O}C to preserve their structural integrity and avoid aggregation until they could be used in prospective experiments. This biogenic synthesis strategy eliminates the need for dangerous chemicals and makes use of bioactive materials present in *C. felina* leaves which demonstrates the value of plant-mediated nanoparticles synthesis in the fields of nanotechnology and biomedicine **(Fig3).**

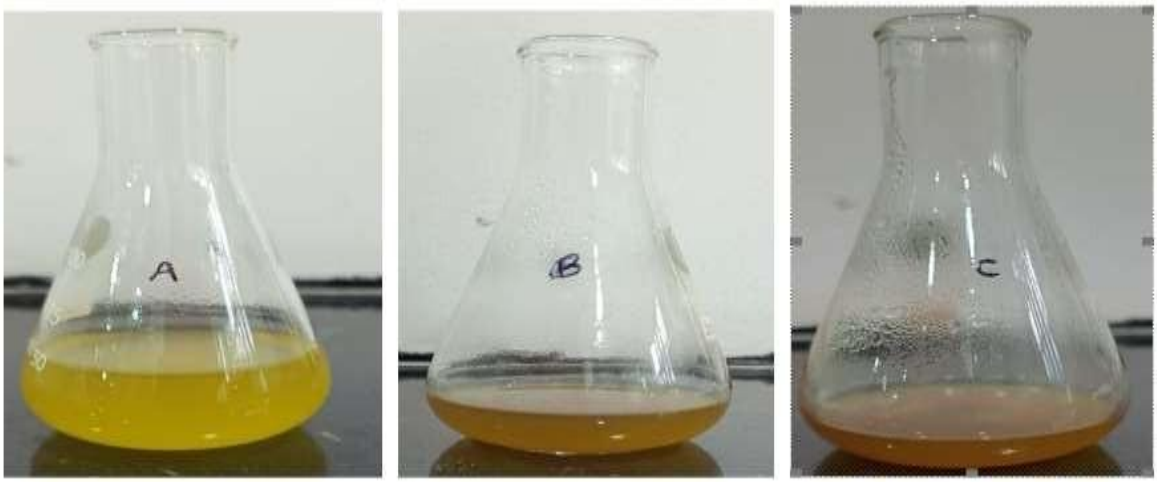

Fig:3. Synthesis of Ag-NPs from C. *felina*

UV-Visible spectroscopy analysis of AgNPs-CFL

The kind of study and report presented on UV-Vis spectrophotometric analysis probably defines the measurement of the silver nanoparticles (AgNPs) produced by *Cleome felina*. With an eye toward the absorption properties of the silver nanoparticles, the scan spans 190 nm to 1100 nm. With a peak absorbance of 3.993, the scan displays a somewhat strong absorption peak at 302 nm. That peak proposes the surface plasmon resonance (SPR) of silver nanoparticles, one of the main characteristics in the spectra of nanomaterials. The data related to absorption suggests that the nanoparticles have an optical signature, very often observed is their presence which AUV-1800 spectrometer was used in the measurement with absorbance settings, average rate of scan speed coming to standard for precision and reliability for this kind of examinations is, the concentration level of the nanoparticles in measure that was done. Regarding the size and concentration determination of the nanoparticles, optical parameters of these studies seek for exactness. Important for hydrogenels, the monitoring range spans both UV and visible light wavelengths with Paleolithic characteristics reminiscent of the silver nanoparticles. The upper limit is 1100 nm and it is 190 nm. The occurrences accompanying the peak imply that the investigated silver nanoparticles have unique size **(Fig4).**

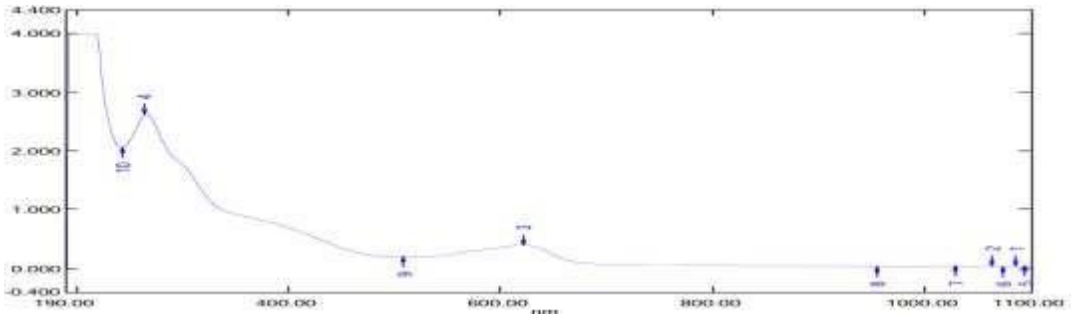

Fig.4: UV-Visible spectroscopy analysis of AgNPs-CFL

FT-IR Characterization of Silver Nanoparticles from *C. felina* (CFL-AgNPs)

The FTIR spectrum of the silver nanoparticles developed from *Cleome felina* shows several unique peaks connected to different functional groups. Together with the stabilizing agents, this offers some insight into the potential chemistry of the nanoparticles. The presence of hydroxyl groups is indicated by a large peak at 3602.16 cm^{-1} with a base at 3600 cm^{-1} because of hydroxyl stretch. This could be because the plant extract contains water molecules or chemicals that include hydroxyl. Because of the N-H stretch, which is characteristic of proteins or other nitrogenous components of the extract or stabilizing agents, the peak corresponding to amine groups is 3143.39 cm^{-1}. Around 3148.60 cm-1, a second C-H stretch is observed,

which is caused by alkyl groups. This suggests that the entire region may be composed of organic molecules or aliphatic hydrocarbons. Strong peaks at 2970.87 cm-1 and 2866.67 cm-1, which correspond to the C-H stretch of aliphatic organic stabilizers of the nanoparticles or other organic components of the plant extract, further support these C-H stretches.

Additionally, a C=O stretch is observed at 1601.59 cm^{-1}, which may be connected to the carbonyl components of carboxylic acids or esters that help stabilize the nanoparticles. This information about ammonia-bearing compounds possibly from amino acids or parts of proteins found in the *C. felina* extract that support the creation and stabilization of the nanoparticles is further supported by the N-H bending at 1377.89 cm^{-1}. At 1193.72 cm^{-1} and 1067.76 cm^{-1}, two peaks linked to C-N stretches indicate the presence of nitrogen-bearing functional groups that could represent proteins or other organic compounds acting as capping agents. A C-O stretch linked to alcohols, ethers, or esters components of the organic matrix that are thought to stabilize the silver nanoparticles is represented by the peak at 1141.65 cm-1. The existence of organic components that might be utilized for stabilizing or capping the nanoparticles is further confirmed by the C-H bending observed at the C-H stretching frequencies at 1004.73 cm^{-1} and 704.65 cm-1, which are connected to the alkyl groups' in-plane vibrations.

Numerous functional groups, including hydroxyl, amine, alkyl, carbonyl, and even nitrogenous groups, are generally detected by FTIR analysis. These are all especially crucial for the reduction, stability, and functionalization of silver nanoparticles made with *Cleome felina***(Fig5).**

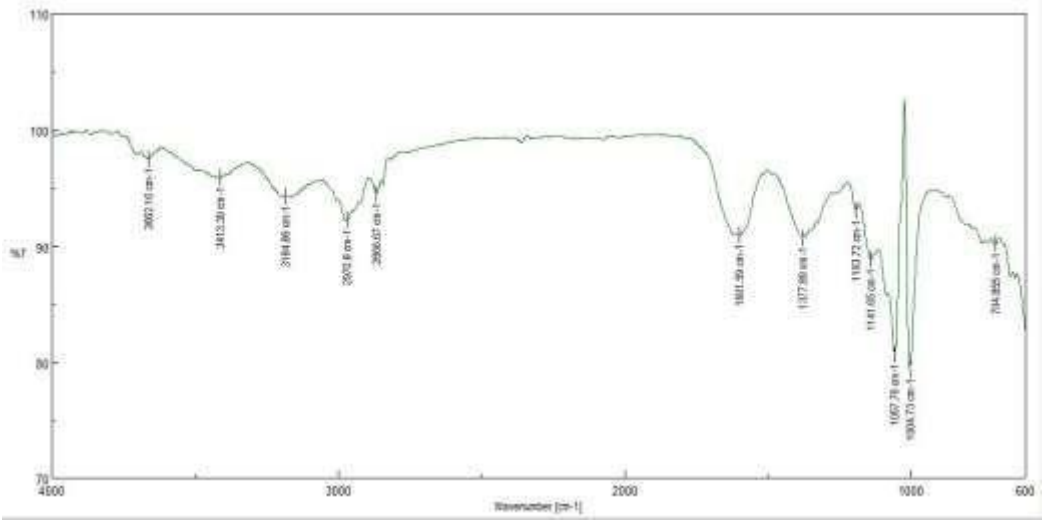

Fig.5: FT-IR Characterization of Silver Nanoparticles from *C. felin*a (CFL-AgNPs)

Scanning Electron Microscope (SEM) analysis of AgNPs -CFL

The scanning electron microscopy (SEM) analysis of silver nanoparticles (AgNPs) synthesized from *C. felina* demonstrated irregularly shaped nanostructures exhibiting various morphologies. The micrographs, taken at magnifications between 7.00kX and 7.50kX, displayed nanoparticles characterized by a mix of rough, aggregated structures and comparatively well-dispersed particles. The 5.00 µm scale bar indicates that the nanoparticles are within the nanometer to sub-micrometer range. Morphological analysis revealed a heterogeneous population, with certain particles exhibiting well-defined crystalline structures, whereas others showed a rough polycrystalline texture, indicating a potential face-centered cubic (FCC) lattice structure characteristic of AgNPs.

Agglomeration occurred in specific regions, likely due to electrostatic interactions or inadequate stabilization during the synthesis process. The presence of well-dispersed nanoparticles suggests partial stabilization. The analysis of surface texture revealed non-uniformity, characterized by variations in roughness and shape, including both plate-like structures and more rugged formations. The presence of both isolated and clustered

nanoparticles indicates that the synthesis method produced a heterogeneous distribution of particle sizes and morphologies **(Fig6).**

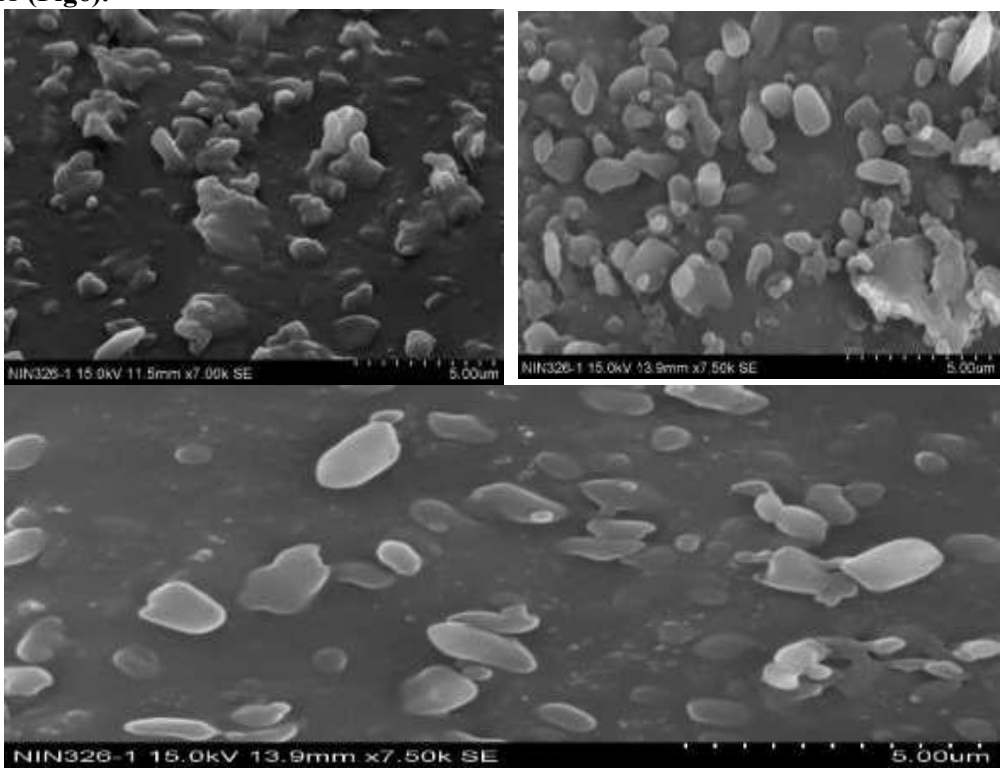

Fig.6: Scanning Electron Microscope (SEM) analysis of AgNPs -CFL

Transmission Electron Microscopy analysis of AgNPs -CFL

The TEM analysis of CFL AgNPs revealed key morphological features such as size, shape, and dispersion. The images showed nanoscale CA-AgNPs with an average diameter of 15 nm, confirming their small and uniform nature. The synthesized CA-AgNPs had a monoclinic structure, a polydisperse distribution, and were mainly spherical, indicating some variation in particle distribution while mostly maintaining a round shape. The imaging results suggest that the nanoparticles were evenly dispersed with minimal aggregation, highlighting their stability and suitability for various applications, including biological and nanotechnological fields **(Fig7).**

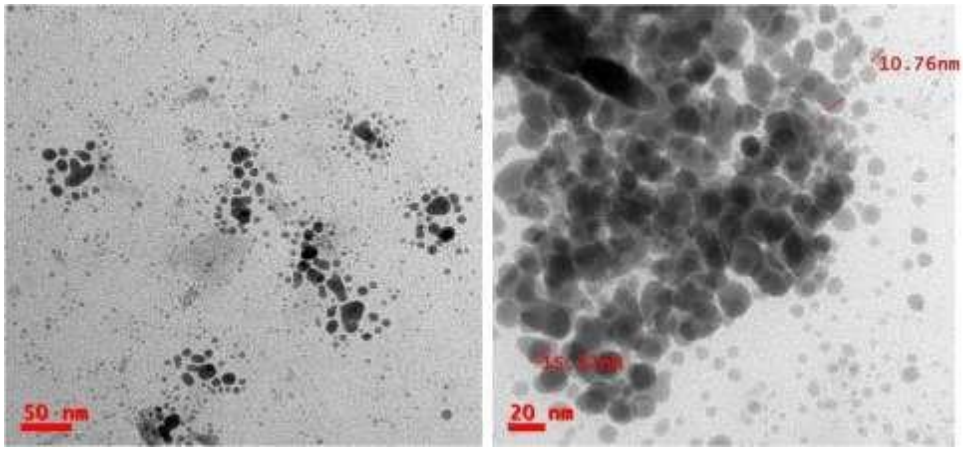

Fig.7: Transmission Electron Microscopy analysis of AgNPs -CFL

XRD Spectra of *C. felina* silver nanoparticles (CFL-AgNPs)

The X-ray diffraction (XRD) examination of silver nanoparticles (AgNPs) synthesized with *C. felina* was conducted using a Bruker D8 Advance LYNXEYE XE-T diffractometer at the CSIR-Indian Institute of Chemical Technology, Hyderabad. The diffraction pattern was captured over a 2θ range of 2.000° to 79.995°, utilizing a step size of 0.020° and a scan duration of 0.30 seconds per step. The equipment functioned at 40.0 kV and 31.0 mA utilizing a Cu Kα1 radiation source (λ = 1.54060 Å). The resulting diffractogram exhibited distinct peaks at 23.500°, 27.265°, 27.712°, 28.239°, 29.669°, 32.179°, 32.662°, 39.234°, 40.449°, 41.166°, 43.103°, 46.155°, and 50.079° throughout the 2θ range, correlating to interplanar spacings (d-values) from 3.78258 Å to 1.82000 Å. The most pronounced relative intensity peak was at 27.265° (d = 3.26827 Å), signifying a robust diffraction signal. The existence of several diffraction peaks indicates the crystalline characteristics of the synthesized AgNPs, presumably displaying a face-centered cubic (FCC) structure, characteristic of metallic silver. The agglomeration or variations in crystallite size may have influenced the widening and intensity fluctuations of the peaks **(Fig8).**

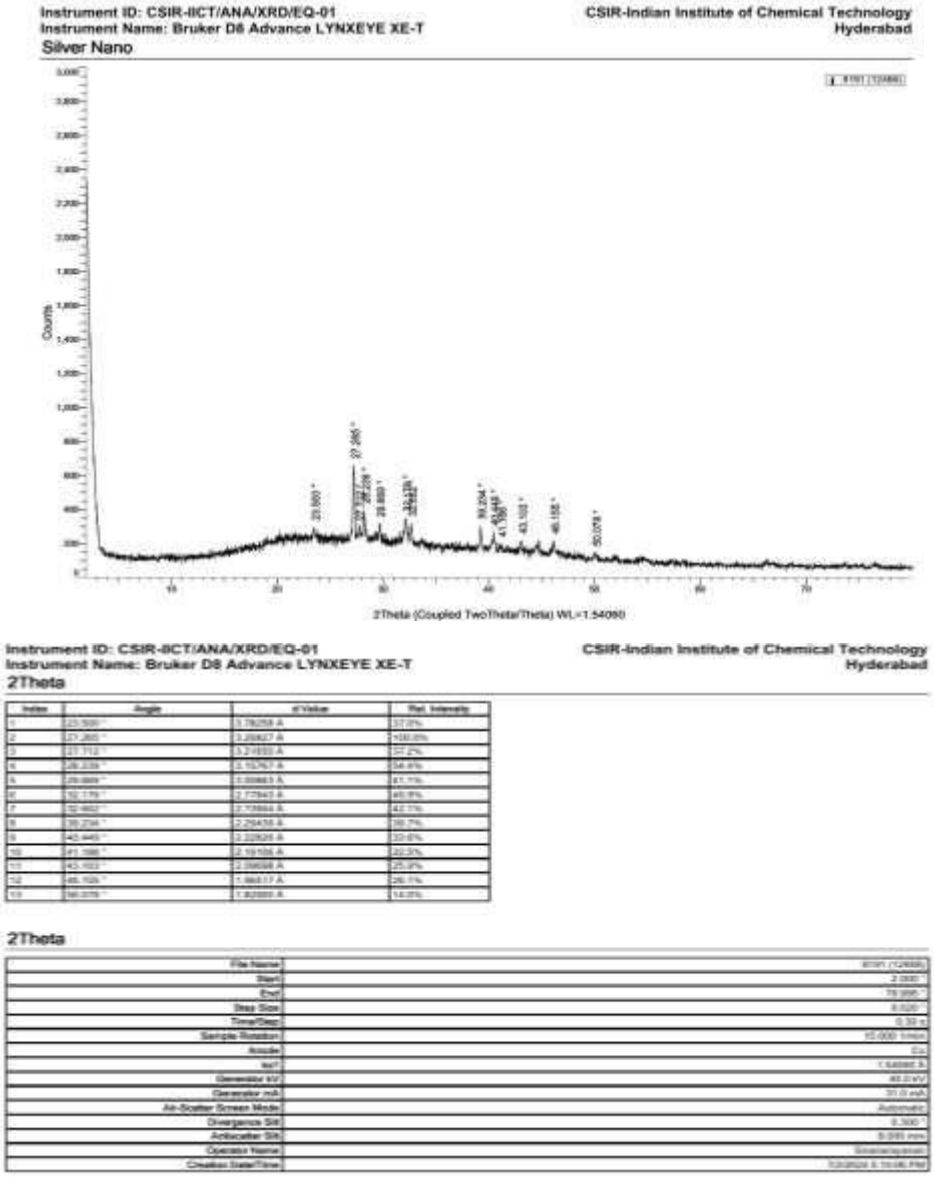

Fig.8: XRD Spectra of *C. felina* silver nanoparticles (CFL-AgNPs**)**

Characterization of CFL -AgNPs using Zeta Potential

The characterization of silver nanoparticles (AgNPs) synthesized using *C. felina* (CFL-AgNPs) was conducted through zeta potential analysis to evaluate their colloidal stability and surface charge. The zeta potential measurement was performed at a temperature of 25.0°C, with the dispersion medium exhibiting a viscosity of 0.895 mPa·s and a conductivity of 0.726 mS/cm under an electrode voltage of 3.3 V. The results indicate a mean zeta potential value of -2.0 mV, suggesting weak electrostatic repulsion among the nanoparticles. This relatively low zeta potential value implies a tendency toward agglomeration due to insufficient charge stabilization, which could influence the long-term stability of the colloidal suspension. The electrophoretic mobility mean was recorded at -0.000015 cm2/Vs, further supporting the observation of weak surface charge distribution. The corresponding zeta potential distribution graph demonstrates a sharp peak centered around -2.0 mV, reflecting a uniform but low charge distribution across the nanoparticle population. Given these findings, further surface modifications or stabilizing agents may be required to enhance the colloidal stability of CFL-AgNPs for potential biomedical or environmental applications **(Fig 9).**

202404101610000.nzt

Measurement Results

Date	: 10 April 2024 16:10:11
Measurement Type	: Zeta Potential
Sample Name	: BSANP-15BSA+20PX-ZETA
Temperature of the holder	: 25.0 deg. C
Viscosity of the dispersion medium	: 0.895 mPa.s
Conductivity	: 0.726 mS/cm
Electrode Voltage	: 3.3 V

Calculation Results

Peak No.	Zeta Potential	Electrophoretic Mobility
1	-2.0 mV	-0.000015 cm2/Vs
2	— mV	— cm2/Vs
3	— mV	— cm2/Vs

Zeta Potential (Mean)	: -2.0 mV
Electrophoretic Mobility mean	: -0.000015 cm^2/Vs

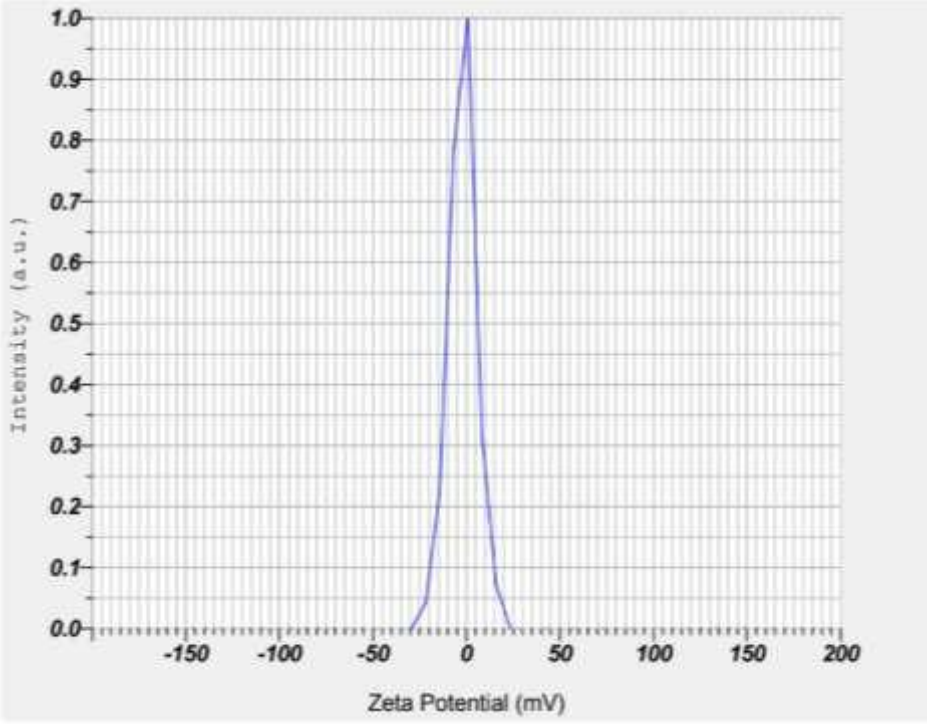

Fig.9: Zeta potential Spectra of *C. felina* silver nanoparticles (CFL-AgNPs**)**

Antibacterial activity

The antibacterial properties of silver nanoparticles (AgNPs) made from the leaves of the *C. felina* plant have been examined utilizing the Agar well-diffusion method. Four distinct concentrations (25, 50, 75, and 100 µg/µL) have been assessed utilizing ampicillin as the reference antibiotic. The inquiry specifically focused on harmful bacteria, including *Staphylococcus aureus*, *Escherichia coli*, *Streptococcus pneumoniae*, and *Pseudomonas aeruginosa*.

Antibacterial activity of *C. felina*- AgNPs

The antibacterial efficacy of silver nanoparticles (AgNPs) derived from the leaves of the *C. felina* plant was assessed utilizing the agar well-diffusion technique, with ampicillin as the control antibiotic. The research examined the antibacterial effectiveness of four distinct concentrations (25, 50, 75, and 100 µg/µL) of *C. felin*a-derived silver nanoparticles (CFL-AgNPs) against four bacterial strains: *Staphylococcus aureus*, *Escherichia coli*, *Streptococcus pneumoniae*, and *Pseudomonas aeruginosa*. The zone of inhibition, quantified in mm, was documented at each concentration to assess the efficacy of the nanoparticles relative to ampicillin. Ampicillin exhibited inhibition zones of 14 mm, 16 mm, 17 mm, and 19 mm against *Staphylococcus aureus* at increasing concentrations, whereas CFL-AgNPs displayed lesser nevertheless significant inhibitory effects, with zones of 8 mm, 9 mm, 10 mm, and 12 mm, respectively. *E. coli* had a marginally enhanced response to both ampicillin (14 mm to 20 mm) and CFL-AgNPs (9 mm to 14 mm) with increasing concentration. The inhibition zones for *Streptococcus pneumoniae* subjected to CFL-AgNP treatment varied from 6 mm at the lowest concentration to 11 mm at the maximum, signifying a moderate antibacterial efficacy. *Pseudomonas aeruginosa* exhibited inhibitory zones measuring 7 mm, 9 mm, 11 mm, and 14 mm in response to escalating concentrations of CFL-AgNPs. The results indicate that whereas ampicillin shown greater antibacterial efficacy, silver nanoparticles produced from *C. felina* also showed a dose-dependent inhibitory impact, especially against *E. coli* and *Pseudomonas aeruginosa*, positioning them as a possible alternative antimicrobial agent.

Sr. No	**Bacterial Strain**	**Ampicillin**				***Con. (µg). of C. felina silver nanoparticles (*CFL-AgNPs*)***			
		Concentration (µg/ml)							
		25	**50**	**75**	**100**	**25**	**50**	**75**	**100**
		Zone of Inhibition represented in mm							
1.	*Staphylococcus aureus*	14	16	17	19	8	9	10	12
2.	*E. coli*	14	16	18	20	9	11	12	14
3.	*Streptococcus pneumonia*					6	8	9	11
4.	*Pseudomonas aeruginosa*					7	9	11	14

The comparative analysis suggests that CFL-AgNPs exhibit moderate antibacterial activity, although their effect was slightly lower than that of ampicillin. The concentration-dependent trend indicates that the nanoparticles' antimicrobial activity could be attributed to their interaction with bacterial membranes, leading to cell damage. Among the tested strains, *E. coli* and *P. aeruginosa* displayed the highest susceptibility, whereas *S. pneumoniae* was the least affected. These findings suggest that CFL-AgNPs hold promise as antimicrobial agents and could be further explored for therapeutic applications **(Table 1& Fig 10,11)**

Table .1: Anti-Bacterial Activity of Standard Ampicillin and CFL-AgNPs

Fig.10: Anti-Bacterial Activity of Standard Ampicillin **(A)** *Staphylococcus aureus* **(B)** *E. coli*

Fig.11: Anti-Bacterial Activity of CFL Silver nano particle(A) *Staphylococcus aureus* (B) *E. coli* (C) *Streptococcus pneumonia* (D) *Pseudomonas aeruginosa*

Minimum Inhibitory Concentration (MIC) of Ampicillin and *C. felina* silver nanoparticles (POL-AgNPs)

The Minimum Inhibitory Concentration (MIC) is defined as the lowest concentration of an antimicrobial agent required to prevent the visible growth of a microorganism after overnight incubation. In this study, the MIC values for both ampicillin and *C. felina*-derived silver nanoparticles (CFL-AgNPs) were assessed against

four bacterial strains: *Staphylococcus aureus, Escherichia coli, Streptococcus pneumoniae*, and *Pseudomonas aeruginosa*.

The results indicate that CFL-AgNPs exhibited antibacterial activity at a concentration of 200 µg/mL against all tested bacterial strains, confirming their potential as an alternative antimicrobial agent. The zone of inhibition values recorded at different concentrations highlight the comparative effectiveness of CFL-AgNPs against these bacteria. For *S. aureus*, ampicillin demonstrated decreasing activity with increasing concentration, with zone values ranging from 0.329 mm at 5 µg/mL to 0.104 mm at 200 µg/mL. CFL-AgNPs, however, maintained a more stable inhibitory effect, showing a gradual decrease from 0.374 mm at 5 µg/mL to 0.214 mm at 200 µg/mL. *E. coli* followed a similar trend, with ampicillin displaying a decreasing inhibition effect from 0.319 mm at 5 µg/mL to 0.108 mm at 200 µg/mL, whereas CFL-AgNPs showed a slightly better response, with inhibition zones ranging from 0.371 mm to 0.143 mm.

In the case of *S. pneumoniae* and *P. aeruginosa*, CFL-AgNPs exhibited considerable antibacterial efficacy. The inhibition zone values for *S. pneumoniae* increased with concentration, ranging from 0.376 mm at 5 µg/mL to 0.406 mm at 200 µg/mL. *P. aeruginosa* followed a similar pattern, with the inhibition zone increasing from 0.389 mm to 0.412 mm, indicating that CFL-AgNPs were effective against these bacteria even at higher concentrations. These results suggest that CFL-AgNPs demonstrated a significant bacteriostatic effect, particularly against *S. pneumoniae* and *P. aeruginosa*, which exhibited consistent or improved inhibition at increasing concentrations.

Overall, the study highlights that while ampicillin exhibited antimicrobial activity, its effectiveness reduced as concentration increased. In contrast, CFL-AgNPs maintained a more consistent inhibitory effect, suggesting a potential role as an alternative antibacterial agent. These findings support further investigation into CFL-AgNPs as a promising candidate for combating antibiotic-resistant bacterial strains **(Table 2 & Fig 12,13).**

Table.2: Minimum Inhibitory Concentration (MIC) of Ampicillin and CFL-AgNPs

S. No	**Bacteria**	**Ampicillin**						***Con. (µg). of C. felina silver nanoparticles* (CFL-AgNPs)**					
		Concentration (µg/mL)											
		5	**10**	**25**	**50**	**100**	**200**	**5**	**10**	**25**	**50**	**100**	**200**
		Zone of Inhibition represented in mm											
1.	*S. aureus*	0.329	0.303	0.256	0.249	0.181	0.104	0.374	0.332	0.313	.276	0.251	0.214
2.	*E. coli*	0.319	0.297	0.283	0.264	0.196	0.108	0.371	0.326	0.284	0.242	0.182	0.143
3.	*S. pneumoniae*							0.376	0.387	0.391	0.371	0.358	0.406
4.	*P. aeruginosa*							0.389	0.373	0.386	0.373	0.390	0.412

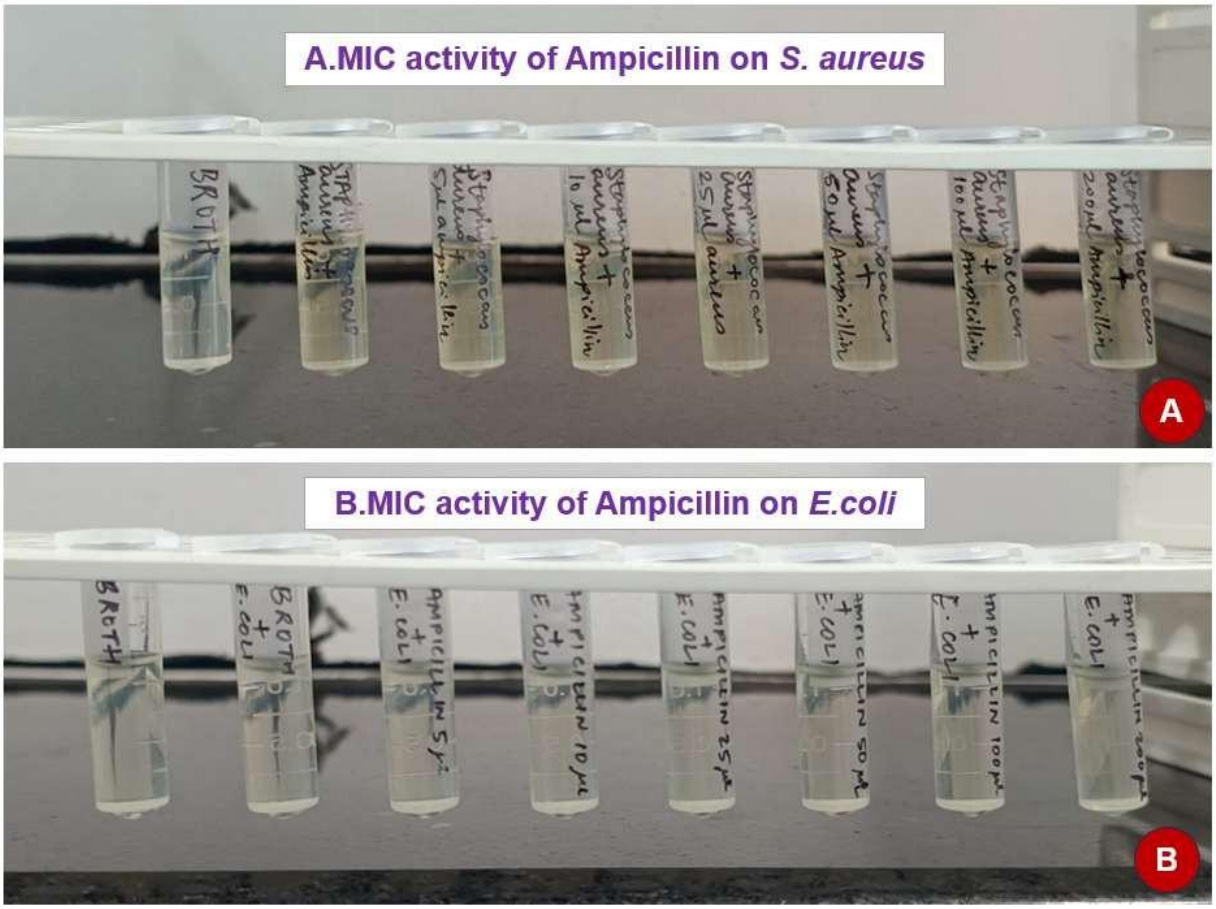

Fig:12AB. MIC activity of Ampicillinn on *S.aureus* and *E.coli*

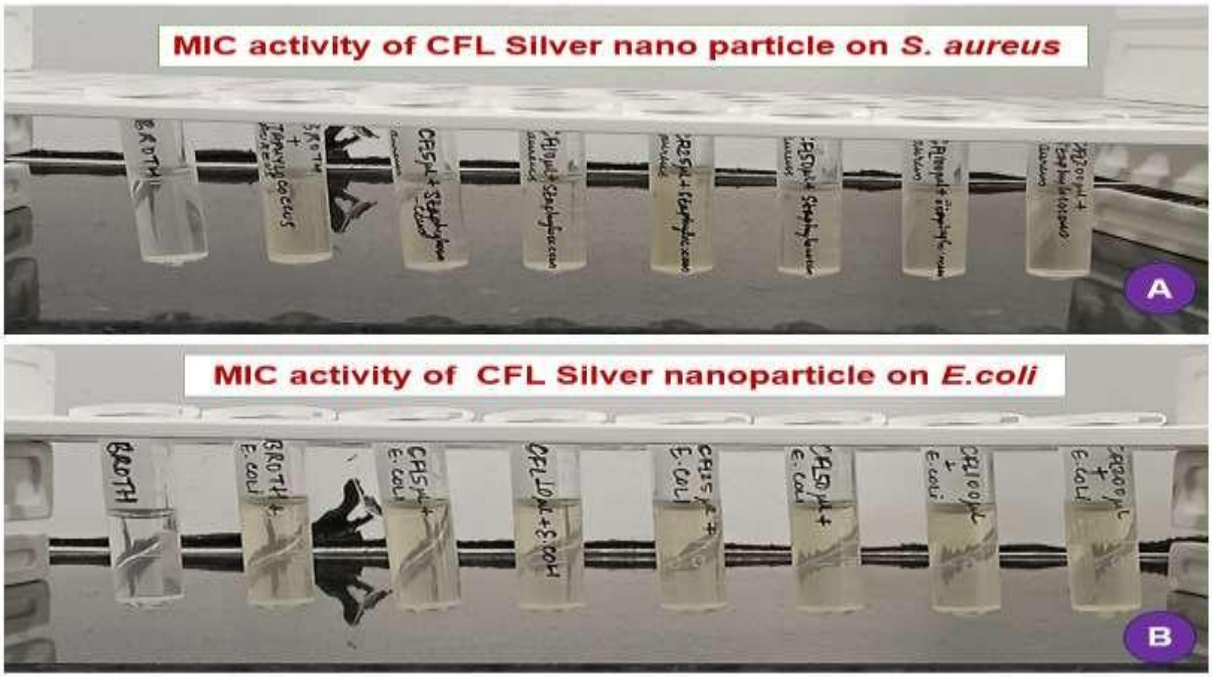

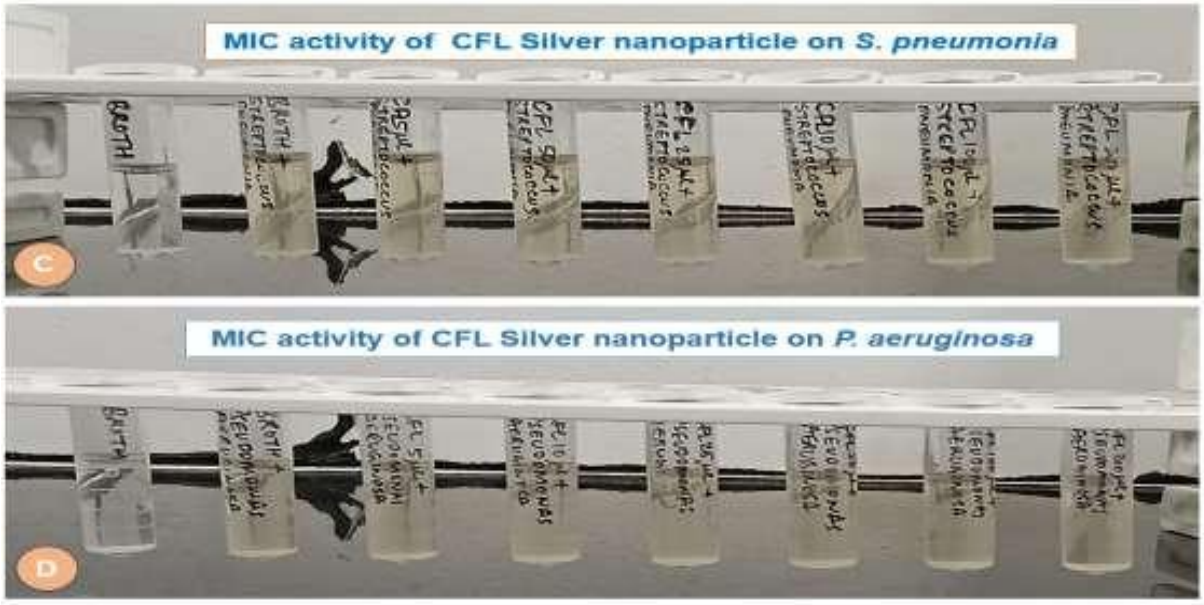

Fig:13A-D. MIC activity of CFL-AgNPs on *S.aureus* , *E.coli, S. pneumoniae& P. aeruginosa*

Antifungal activity of Fluconazole and CFL-AgNPs

The antifungal efficacy of CFL-AgNPs was assessed against *Candida albicans* and *Aspergillus niger* via the well diffusion technique on Sabouraud Dextrose Agar (SDA). The findings exhibited a concentration-dependent augmentation in the zone of inhibition for both fungal strains. CFL-AgNPs demonstrated inhibitory zones of 4 mm, 6 mm, 9 mm, and 13 mm against *Candida albicans* at doses of 25, 50, 75, and 100 µg/ml, respectively. In contrast, fluconazole, a conventional antifungal agent, exhibited greater inhibition zones of 9 mm, 11 mm, 13 mm, and 16 mm at same dosages. For *Aspergillus niger,* CFL-AgNPs demonstrated inhibition zones of 3 mm, 3.5 mm, 5.4 mm, and 8 mm, whereas fluconazole showed inhibition zones of 11 mm, 14 mm, 19 mm, and 24 mm at the respective concentrations. The data suggest that although CFL-AgNPs exhibit antifungal capabilities, their effectiveness is inferior to that of fluconazole at equivalent concentrations. The observed inhibition indicates that CFL-AgNPs may be investigated as potential antifungal medicines, either independently or in conjunction with current antifungal medications, to augment their efficacy **(Table 3& Fig 14,15).**

Table.3: Antifungal activity of Fluconazole and CFL-AgNPs

S. No	**Fungal Strains**	**Fluconazole**				***Con. (µg). of C. felina silver nanoparticles (***CFL -AgNPs)			
Concentration (µg/ml)									
		25	**50**	**75**	**100**	**25**	**50**	**75**	**100**
		Zone of inhibition (mm)							
1	*Candida albicans*	9	11	13	16	4	6	9	13
2	*Aspergillus niger*	11	14	19	24	3	3.5	5.4	8

International Journal of Environmental Sciences
ISSN: 2229-7359
Vol. 11 No. 17s,2025
https://theaspd.com/index.php

Fig.14: Anti-fungal Activity of Fluconozole **A.** *Candida albicans* **B.** *Aspergillus niger*

Fig.15: Anti-fungal Activity of CFL Silver nano particle.**A.***C. albicans* **B.** *A. niger*

DISCUSSIONS

The *Cleome felina is* annual herb, it is belonging to the family Cleomaceae, which is a medicinal plant and is endemic to peninsular India (Hanumantha Rao, 2016). It is annual hairy herb is 30–60 cm, with trifoliate leaves, corolla pink, and more than 50 stamens; seedpods with seeds are slightly longer than the pedicel and is widely distributed in Deccan districts of Madras Presidency. (Joseph et al., 2014). The present study of synthesis of the *Cleome felina* leaf AgNPs during the reduction process is indicated by change in the color of the reaction solution from yellow to dark brown which can be visually observed. The synthesized silver nano particles from *C. felina* (AgNPs), its characterization through FTIR, the major peaks absorptions are observed at hydroxyl groups is indicated by a large peak at 3602.16 cm^{-1}, amine groups is 3143.39 cm^{-1}, C=O stretch is observed at 1601.59 cm^{-1}, C=O stretch is observed at 1601.59 cm^{-1}, and N-H bending at 1377.89 cm^{-1}. At 1193.72 cm^{-1}. UV-vis spectroscopy is an effective and dependable method for the first characterisation of produced nanoparticles, as well as for monitoring the synthesis and stability of AgNPs [Sastry et al., 1998]. Silver nanoparticles (AgNPs) possess distinctive optical characteristics that enable them to interact intensely

with particular wavelengths of light [Madhu Yadav et al., 2018]. The present study UV-Vis spectrophotometric analysis substantiated the existence of silver nanoparticles (AgNPs) derived from *C. felina*, characterized by a pronounced absorption peak at 302 nm and a peak absorbance of 3.993, signifying surface plasmon resonance (SPR). The absorption data substantiates their unique optical signature, emblematic of AgNPs. Scanning Electron Microscopy (SEM) is a surface imaging technique adept in distinguishing various particle sizes, size distributions, nanomaterial geometries, and the surface morphology of manufactured particles at micro and nanoscale levels.Fissan et al., (2014; Hall, 2007). The current SEM examination of AgNPs derived from *C. felina* demonstrated irregular nanostructures exhibiting diverse morphologies, comprising coarse aggregates and uniformly dispersed particles. The nanoparticles, observed at 7.00kX–7.50kX magnification, ranged from nanometer to sub-micrometer sizes. Morphological evaluation revealed a diverse population, characterized by crystalline and polycrystalline structures indicative of a face-centered cubic lattice. Surface analysis revealed irregularities. TEM is a significant and commonly employed technology for the evaluation of nanomaterials, utilized to get quantitative assessments of particle and/or grain size, size distribution, and shape [Lin et al., 2014]. The magnification of a Transmission Electron Microscope (TEM) is primarily dictated by the ratio of the distance from the objective lens to the specimen and the distance from the objective lens to its image plane. Williams et al. (2019)

Present studies of TEM analysis showed CFL AgNPs' size, shape, and dispersion. The scans showed nanoscale CA-AgNPs with an average diameter of 15 nm, demonstrating their uniformity. The synthesized CA-AgNPs were monoclinic, polydisperse, and predominantly spherical, exhibiting particle distribution variation but maintain a round shape. The XRD analysis of *C. felina* resulting diffractogram exhibited distinct peaks at 23.500°, 27.265°, 27.712°, 28.239°, 29.669°, 32.179°, 32.662°, 39.234°, 40.449°, 41.166°, 43.103°, 46.155°, and 50.079° throughout the 2θ range, correlating to interplanar spacings (d-values) from 3.78258 Å to 1.82000. The calculated XRD values with JCPDS Card No. 04-0783 are consistent with certain previously published results, by Mahajan et al., (2019). The zeta potential of silver nanoparticles (CFL-AgNPs) is -2.0 mV, indicating weak electrostatic repulsion and agglomeration, suggesting surface modifications or stabilizers may enhance colloidal stability.

The silver nanoparticles (AgNPs) are well-known as the most universal antimicrobial substances due to their strong biocidal effect against microorganisms, which has been used for over the past decades to prevent and treat various diseases (Oei et al., 2012). AgNPs are also widely used as anti-fungal (Kim et al., 2009), anti-inflammatory (Nadworny et al., 2010). AgNPs have exhibited highly antibacterial action against multiple Gram-positive and Gram-negative bacteria (Cavassin et al., 2015). In this study, the bacterial strains Gram positive of *Staphylococcus aureus* (ATCC 25923)*, Streptococcus pneumonia* (ATCC 33400)*,* and Gram negative of Pseudomonas *aeruginosa* (ATCC 27853), *E. coli* (ATCC 25922) used in the study were obtained from ATCC. The CFL -AgNPs as an antimicrobial agent and the comparative antibacterial studies with ampicillin used as standard drug, the strongest inhibition seen against E. coli (14 mm) and P. aeruginosa (14 mm) at maximal concentration, CFL-AgNPs showed dose-dependent antibacterial efficacy. Although ampicillin showed better efficiency generally, CFL-AgNPs showed notable inhibition, implying their possible use as a substitute antibacterial drug especially against Gram-negative bacteria. These results show its exciting relevance in therapeutic uses.

The minimum inhibitory concentration (MIC) values of ampicillin and *C. felina*-derived silver nanoparticles (CFL-AgNPs) against four bacterial strains *S. aureus, E. coli*, *S. pneumoniae*, and *P. aeruginosa* were evaluated in this work. Against all studied strains, results revealed that CFL-AgNPs displayed antibacterial action at a concentration of 200 µg/mL. With rising concentration, CFL-AgNPs showed a slow decline in their more consistent inhibitory impact. With steady or better inhibition at increasing concentrations, CFL-AgNPs shown rather strong antibacterial effectiveness in the cases of *S. pneumoniae* and *P. aeruginosa*.

Nanoparticles, such as silver nanoparticles (AgNPs), have been used for a long time as antimicrobial agents and are highly effective against fungal pathogens (Silva et al., 2017; Salem et al., 2022). The results indicated the maximum inhibition seen against *Candida albicans* (13 mm) and *Aspergillus niger* (8 mm) at 100

µg/ml, CFL-AgNPs shown dose-dependent antifungal efficacy. Although fluconazole proved to be more effective, CFL-AgNPs showed notable inhibition, implying their possible use as either alternative or supplementary antifungal drugs for more therapeutic uses.
Abbreviations: CFL: *Cleome felina* leaf**; AgNPs:** Silver nano particles.

CONCLUSIONS

The study successfully synthesized and analyzed silver nanoparticles generated from *Cleome felina* (CFL-AgNPs), validating their structural, optical, and antibacterial attributes. UV-Vis examination indicated a pronounced SPR peak at 302 nm, whilst SEM and TEM imaging validated a monoclinic, polydisperse, and mostly spherical morphology with an average diameter of 15 nm. CFL-AgNPs demonstrated a dose-dependent antibacterial effect, with maximal inhibition recorded against *E. coli* (14 mm) and *P. aeruginosa* (14 mm), indicating their potential as an alternative antimicrobial agent, especially against Gram-negative bacteria. CFL-AgNPs exhibited antifungal efficacy, achieving maximal inhibition of 13 mm against *Candida albicans* and 8 mm against *Aspergillus niger*. Although less efficacious than fluconazole, their inhibitory properties indicate possible applications in antifungal treatment. These findings underscore CFL-derived nanoparticles as viable candidates for antibacterial applications, necessitating further exploration of their modes of action and therapeutic potential.

REFERENCES

1. Kumar, R., Ghoshal, G., Jain, A., & Goyal, M. (2017). Rapid green synthesis of silver nanoparticles (AgNPs) using (Prunus persica) plants extract: exploring its antimicrobial and catalytic activities. *J. Nanomed. Nanotechnol*, *8*(4), 1-8.
2. Balachandar, R., Gurumoorthy, P., Karmegam, N., Barabadi, H., Subbaiya, R., Anand, K., ... & Saravanan, M. (2019). Plant-mediated synthesis, characterization and bactericidal potential of emerging silver nanoparticles using stem extract of Phyllanthus pinnatus: a recent advance in phytonanotechnology. *Journal of Cluster Science*, *30*, 1481-1488.
3. Quazi, S., Rodrigo, S., Fatima, Z., & Prakash, A. (2023). Nanoparticles: Types, Applications, and Commercial Products. In *Implications of Nanoecotoxicology on Environmental Sustainability* (pp. 15-41). IGI Global.
4. Singh, A. V., Ansari, M. H. D., Laux, P., & Luch, A. (2019). Micro-nanorobots: important considerations when developing novel drug delivery platforms. *Expert opinion on drug delivery*, *16*(11), 1259-1275.
5. Yaqoob, A. A., Parveen, T., Umar, K., & Mohamad Ibrahim, M. N. (2020). Role of nanomaterials in the treatment of wastewater: A review. *Water*, *12*(2), 495.
6. Khan, I., Saeed, K., & Khan, I. (2019). Nanoparticles: Properties, applications and toxicities. *Arabian journal of chemistry*, *12*(7), 908-931.
7. Baig, N., Kammakakam, I., & Falath, W. (2021). Nanomaterials: A review of synthesis methods, properties, recent progress, and challenges. *Materials advances*, *2*(6), 1821-1871.
8. Sabouri, Z., Fereydouni, N., Akbari, A., Hosseini, H. A., Hashemzadeh, A., Amiri, M. S., ... & Darroudi, M. (2020). Plant-based synthesis of NiO nanoparticles using salvia macrosiphon Boiss extract and examination of their water treatment. *Rare Metals*, *39*(10), 1134-1144.
9. Tulli, F. et al. (2022). Synthesis, properties, and uses of silver nanoparticles obtained from leaf extracts. In Green Synthesis of Silver Nanomaterials*, Elsevier*.
10. Zahra, Z., Habib, Z., Chung, S., & Badshah, M. A. (2020). Exposure route of TiO2 NPs from industrial applications to wastewater treatment and their impacts on the agro-environment. *Nanomaterials*, *10*(8), 1469.
11. Rassaei, L., Marken, F., Sillanpää, M., Amiri, M., Cirtiu, C. M., & Sillanpää, M. (2011). Nanoparticles in electrochemical sensors for environmental monitoring. *TrAC Trends in Analytical Chemistry*, *30*(11), 1704-1715.
12. Chen, J., Guo, Y., Zhang, X., Liu, J., Gong, P., Su, Z., ... & Li, G. (2023). Emerging nanoparticles in food: Sources, application, and safety. *Journal of Agricultural and Food Chemistry*, *71*(8), 3564-3582.
13. Rasool, A., Krismastuti, F. S. H., Zulfajri, M., Meliana, Y., & Sudewi, S. (2024). A smart way to increase the growth and productivity of crops through nano-fertilizer. In *Molecular impacts of nanoparticles on plants and algae* (pp. 333-346). Academic Press.
14. Gaonkar, S. R., Kamat, S., Naik, R., & Sagar, A. (2024). Community vs. Hospital-Acquired MDR UTIs in Goa: Challenges in Pathogen Control and Treatment: A Review. *Microbiology Archives, an International Journal*.
15. Islam, F., Shohag, S., Uddin, M. J., Islam, M. R., Nafady, M. H., Akter, A., ... & Cavalu, S. (2022). Exploring the journey of zinc oxide nanoparticles (ZnO-NPs) toward biomedical applications. *Materials*, *15*(6), 2160.
16. Rasool, A., Sri, S., Zulfajri, M., & Krismastuti, F. S. H. (2024). Nature inspired nanomaterials, advancements in green synthesis for biological sustainability. *Inorganic Chemistry Communications*, *169*, 112954.

17. Varadan, V. K., Pillai, A. S., Mukherji, D., Dwivedi, M., & Chen, L. (2010). *Nanoscience and nanotechnology in engineering*. World Scientific Publishing Company.
18. Singh, J., Dutta, T., Kim, K. H., Rawat, M., Samddar, P., & Kumar, P. (2018). 'Green'synthesis of metals and their oxide nanoparticles: applications for environmental remediation. *Journal of nanobiotechnology*, *16*, 1-24.
19. Rajan, R., Chandran, K., Harper, S. L., Yun, S. I., & Kalaichelvan, P. T. (2015). Plant extract synthesized silver nanoparticles: An ongoing source of novel biocompatible materials. *Industrial Crops and Products*, *70*, 356-373.
20. Uddin, M. M., Khan, M. M. I., & Islam, M. T. (2025). Environmental Accounting and Reporting Practices in Bangladesh: Evidence from Cement, Ceramic, IT, and the Jute Industries. *Environmental Reports; an International Journal*.
21. Adeyemi, J. O., Oriola, A. O., Onwudiwe, D. C., & Oyedeji, A. O. (2022). Plant extracts mediated metal-based nanoparticles: Synthesis and biological applications. *Biomolecules*, *12*,
22. Bao, Y., He, J., Song, K., Guo, J., Zhou, X., & Liu, S. (2021). Plant-Extract-Mediated Synthesis of Metal Nanoparticles. *Journal of Chemistry*, *2021*(1), 6562687.
23. Bindhu, M. R., & Umadevi, M. (2015). Antibacterial and catalytic activities of green synthesized silver nanoparticles. *Spectrochimica acta part A: molecular and biomolecular spectroscopy*, *135*, 373-378.
24. Hymavathi, K., & Rani, A. S. (2024). Synthesis and Characterization of Gold Nanoparticles (AuNPs) from Chrozophora rottleri (Geiseler) Spreng. An Evaluation of Antioxidant and Antimicrobial Activities. *Journal of American Medical Science and Research*, 18-53.
25. Marimuthu, S., Rahuman, A. A., Rajakumar, G., Santhoshkumar, T., Kirthi, A. V., Jayaseelan, C., ... & Kamaraj, C. (2011). Evaluation of green synthesized silver nanoparticles against parasites. *Parasitology research*, *108*, 1541-1549.
26. Sharma, V. K., Yngard, R. A., & Lin, Y. (2009). Silver nanoparticles: green synthesis and their antimicrobial activities. *Advances in colloid and interface science*, *145*(1-2), 83-96.
27. Velusamy, P., Das, J., Pachaiappan, R., Vaseeharan, B., & Pandian, K. (2015). Greener approach for synthesis of antibacterial silver nanoparticles using aqueous solution of neem gum (*Azadirachta indica* L.). *Industrial crops and products*, *66*, 103-109.
28. Verma, A., & Mehata, M. S. (2016). Controllable synthesis of silver nanoparticles using Neem leaves and their antimicrobial activity. *Journal of radiation Research and applied sciences*, *9*(1), 109-115.
29. Jain, P. K., Huang, X., El-Sayed, I. H., & El-Sayed, M. A. (2008). Noble metals on the nanoscale: optical and photothermal properties and some applications in imaging, sensing, biology, and medicine. *Accounts of chemical research*, *41*(12), 1578-1586.
30. Chand, J., Panda, S. R., Jain, S., Murty, U. S. N., Das, A. M., Kumar, G. J., & Naidu, V. G. M. (2022). Phytochemistry and polypharmacology of cleome species: A comprehensive Ethnopharmacological review of the medicinal plants. *Journal of Ethnopharmacology*, *282*, 114600.
31. Sirisha, B., Meera, D., & Devi, C. V. (2024). Green Synthesis of Silver, Copper and Bimetallic (Ag-Cu) Nanoparticle using Aqueous Extract of Achyranthes Aspera for Hepatoprotective activity on HEPG2 Cell lines against CCl induced toxicity 4. *Acta Pharma Reports*.
32. Singh, H., Mishra, A., & Mishra, A. K. (2018). The chemistry and pharmacology of Cleome genus: a review. *Biomedicine & Pharmacotherapy*, *101*, 37-48.
33. Hanumantha Rao, V. (2016). Endemic and threatened plants of uranium mining area. *Na. Int. Res. J. Environ. Sci*, *5*, 40-46.
34. Joseph, M., Vincent, A. R., & Charles, A. (2014). The anticancer activity of ethanolic extract of Cleome felina linn. *J. Pharm. Res*, *8*, 1223-1225.
35. Manjuparkavi, K.; Jayanthi, G. (2019). Micromorphological studies of *Cleome felina* L.f. *Int. J. Curr. Res. Biosci. Plant Biol.* , *6*, 32–41.
36. Ugosor, P. T., & Wada, S. T. (2025). Antimicrobial Studies of Biosynthesized Zinc Oxide Nanoparticles. *Microbiology Archives, an International Journal*.
37. Azra, B. H., & Fatima, T. (2024). Zinc nanoparticles mediated by Costus pictus leaf extract to study GC-MS and FTIR analysis. *Plant Science Archives*, *11*, 15.
38. Nadkarni, A. R., (1954). Indian Materia Medica. Vol. 1. Popular Book Depot, Bombay.
39. Henri Baillon, (1874). The Natural History of Plants, Vol. 3. Reeve & Co.
40. Nicola, W. G., Ibrahim, K. M., Mikhail, T. H., Girgis, R. B., & Khadr, M. E. (1996). Role of the hypoglycemic plant extract cleome droserifolia in improving glucose and lipid metabolism and its relation to insulin resistance in fatty liver. *Bollettino Chimico Farmaceutico*, *135*(9), 507-517.
41. Nazneen, S., & Sultana, S. (2024). Green synthesis and characterization of Cissus quadrangularis. L stem mediated zinc oxide nanoparticles. *Plant Sci. Archives*, *1*(05), 10-5147.
42. Shaikh, H. Y., Niazi, S. K., Bepari, A., Cordero, M. A. W., Sheereen, S., Hussain, S. A., Rudrappa, M., Nagaraja, S. K., & Agadi, S. N. (2023). Biological Characterization of *Cleome felina* L.f. Extracts for Phytochemical, Antimicrobial, and Hepatoprotective Activities in Wister Albino Rats. *Antibiotics*, *12*(10), 1506. https://doi.org/10.3390/antibiotics12101506.
43. Anandalakshmi, K., Venugobal, J., & Ramasamy, V. J. A. N. (2016). Characterization of silver nanoparticles by green synthesis method using Pedalium murex leaf extract and their antibacterial activity. *Applied nanoscience*, *6*, 399-408.

44. Pal, S., Tak, Y. K., & Song, J. M. (2007). Does the antibacterial activity of silver nanoparticles depend on the shape of the nanoparticle? A study of the gram-negative bacterium Escherichia coli. *Applied and environmental microbiology*, *73*(6), 1712-1720.
45. Astry M, Patil V, Sainkar SR. (1998). Electrostatically controlled diffusion of carboxylic acid derivatized silver colloidal particles in thermally evaporated fatty amine films. *J Phys Chem B*.;102(8):1404–10. 10.1021/jp9719873.
46. Vanden Bout DA. (2002). Metal nanoparticles: synthesis, characterization, and applications. In: Feldheim DL, Foss CA Jr., editors. New York: Marcel Dekker, c.x + 338 pp. ISBN: 0-8247-0604-8. *J Am Chem Soc* 124:7874–75. 10.1504/IJNT.2011.038201
47. Straková, P., Larmola, T., Andrés, J., Ilola, N., Launiainen, P., Edwards, K., Minkkinen, K., & Laiho, R. (2020). Quantification of Plant Root Species Composition in Peatlands Using FTIR Spectroscopy. *Frontiers in Plant Science*, 11, 597.
48. Pakkirisamy, M Suresh Kumar Kalakandan and Karthikeyen Ravichandran. (2017). Phytochemical screening, GC-MS, FT-IR analysis of methanolic extract of *Curcuma caesia* Roxb (Black Turmeric). *Phcogj.Com*, 9(6):952-956.
49. Eid M. (2022). Characterization of Nanoparticles by FTIR and FTIR-Microscopy. In: Handbook of Consumer Nanoproducts. *Springer*, Singapore. https://doi.org/10.1007/978-981-16-8698 6_89.
50. Pattoo, T. A. (2023). Flora to nano: Sustainable synthesis of nanoparticles via plant-mediated green chemistry. *Plant Science Archives*, 12-17.
51. Ahmed, W., Azmat, R., Mehmood, A., Qayyum, A., Ahmed, R., Khan, S.U., Liaquat, M., Naz, S. and Ahmad, S. (2021). The analysis of new higher operative bioactive compounds and chemical functional group from herbal plants through UF-HPLC-DAD and Fourier transform infrared spectroscopy methods and their biological activity with antioxidant potential process as future green chemical assay. *Arabian Journal of Chemistry*, 14(2), p.102935.
52. Al-Otibi, F. et al. (2021). Biosynthesis of silver nanoparticles using Malva parviflora and their antifungal activity. *Saudi J. Biol. Sci*. 28, 2229–2235.
53. Amargeetha, A., & Velavan, S. (2018). X-ray diffraction (XRD) and energy dispersive spectroscopy (EDS) analysis of silver nanoparticles synthesized from Erythrina indica flowers. *Nanosci. Technol. Open Access*, *5*, 1-5.
54. Nasiriboroumand, M., Montazer, M., & Barani, H. (2018). Preparation and characterization of biocompatible silver nanoparticles using pomegranate peel extract. *Journal of Photochemistry and Photobiology B: Biology*, *179*, 98-104.
55. Kamble, S., Agrawal, S., Cherumukkil, S., Sharma, V., Jasra, R. V., & Munshi, P. (2022). Revisiting zeta potential, the key feature of interfacial phenomena, with applications and recent advancements. *ChemistrySelect*, *7*(1), e202103084.
56. Kibiti CM, Afolayan AJ. (2015). Preliminary Phytochemical Screening and Biological Activities of Bulbine abyssinica Used in the Folk Medicine in the Eastern Cape Province, South Africa. *Evid Based Complement Alternat Med*, 2015:617607.
57. Meri Amerikova, Ivanka Pencheva El-Tibi, Vania Maslarska, Stanislav Bozhanov & Konstantin Tachkov .(2019). Antimicrobial activity, mechanism of action, and methods for stabilisation of defensins as new therapeutic agents, B*iotechnology & Biotechnological Equipment,* 33:1, 671-682, DOI: 10.1080/13102818.2019.1611385.
58. Beata Kowalska-Krochmal, Ruth Dudek-Wicher. (2021). The Minimum Inhibitory Concentration of Antibiotics: Methods, Interpretation, Clinical Relevance. *Pathogens*, 10, 165.
59. Kumar, R., Sharma, P., & Verma, N. (2021). Advances in Transmission Electron Microscopy for Nanoparticle Characterization. Journal of Nanotechnology Research, 15(3), 120–135.
60. Zhang, L., Chen, H., & Li, J. (2020). High-Resolution TEM for Structural Analysis of Metal Nanoparticles. Materials Today Chemistry, 17, 210–225.
61. Singh, D., & Mehta, B. (2019). Morphological Characterization of Silver Nanoparticles Using TEM. International Journal of Nanoscience, 22(4), 455–470.
62. Wang, X., Liu, Y., & Zhou, T. (2018). Application of High-Resolution Transmission Electron Microscopy in Nanotechnology. Nano Letters, 18(7), 7890–7899.
63. Mahajan, P.G.; Dige, N.C.; Vanjare, B.D.; Phull, A.R.; Kim, S.J.; Lee, K.H.(2019). Gallotannin mediated silver colloidal nanoparticles as multifunctional nano platform: Rapid colorimetric and turn-on fluorescent sensor for Hg2+, catalytic and in vitro anticancer activities. *J. Lumin*., 206, 624–633.
64. Sastry, M., Patil, V., & Sainkar, S. R. (1998). Electrostatically controlled diffusion of carboxylic acid derivatized silver colloidal particles in thermally evaporated fatty amine films. *the journal of physical chemistry B*, *102*(8), 1404-1410.
65. Madhu Yadav, Pankaj Baboo, Nisha Gupta, Vandana Arora. (2018). Composition and Characterisation of Argent Nanoparticles and Argent Bionanocomposities. *Asian J. Research Chem.;* 11(5):811-814. doi: 10.5958/0974-4150.2018.00143.8.
66. Lin, P. C., Lin, S., Wang, P. C., & Sridhar, R. (2014). Techniques for physicochemical characterization of nanomaterials. *Biotechnology advances*, *32*(4), 711-726.
67. Williams, D. B., Carter, C. B., Williams, D. B., & Carter, C. B. (2009). *The transmission electron microscope* (pp. 3-22). Springer Us.
68. Fissan, H., Ristig, S., Kaminski, H., Asbach, C., & Epple, M. (2014). Comparison of different characterization methods for nanoparticle dispersions before and after aerosolization. *Analytical Methods*, *6*(18), 7324-7334.
69. Hall, J. B., Dobrovolskaia, M. A., Patri, A. K., & McNeil, S. E. (2007). Characterization of nanoparticles for therapeutics. *Nanomedicine*, *2*(6), 789-803.

70. Cavassin, E. D., de Figueiredo, L. F. P., Otoch, J. P., Seckler, M. M., de Oliveira, R. A., Franco, F. F., ... & Costa, S. F. (2015). Comparison of methods to detect the in vitro activity of silver nanoparticles (AgNP) against multidrug resistant bacteria. *Journal of nanobiotechnology*, *13*, 1-16.

71. Oei, J. D., Zhao, W. W., Chu, L., DeSilva, M. N., Ghimire, A., Rawls, H. R., & Whang, K. (2012). Antimicrobial acrylic materials with in situ generated silver nanoparticles. *Journal of Biomedical Materials Research Part B: Applied Biomaterials*, *100*(2), 409-415.

72. Kim, K. J., Sung, W. S., Suh, B. K., Moon, S. K., Choi, J. S., Kim, J. G., & Lee, D. G. (2009). Antifungal activity and mode of action of silver nano-particles on Candida albicans. *Biometals*, *22*, 235-242.

73. Nadworny, P. L., Wang, J., Tredget, E. E., & Burrell, R. E. (2010). Anti-inflammatory activity of nanocrystalline silver-derived solutions in porcine contact dermatitis. *Journal of inflammation*, *7*, 1-20.

74. Silva, L. P., Silveira, A. P., Bonatto, C. C., Reis, I. G., & Milreu, P. V. (2017). Silver nanoparticles as antimicrobial agents: Past, present, and future. In *Nanostructures for antimicrobial therapy* (pp. 577-596). Elsevier.

75. Salem, S. S., Ali, O. M., Reyad, A. M., Abd-Elsalam, K. A., & Hashem, A. H. (2022). Pseudomonas indica-mediated silver nanoparticles: Antifungal and antioxidant biogenic tool for suppressing mucormycosis fungi. *Journal of Fungi*, *8*(2), 126.